American Mineralogist, Volume 90, pages 1308–1314, 2005

Dehydration processes in the meta-autunite group minerals meta-autunite, metasaléeite, and metatorbernite

YOHEY SUZUKI,[1] TSUTOMU SATO,[2] HIROSHI ISOBE,[3] TOSHIHIRO KOGURE,[4] AND TAKASHI MURAKAMI[4,*]

[1]Frontier Research System for Extremophiles, Japan Marine Science and Technology Center, 2-15, Natsushima-cho, Yokosuka 237-006, Japan
[2]Institute of Nature and Environmental Technology, Kanazawa University, Kanazawa, Ishikawa 920-1192, Japan
[3]Department of Earth Science, Kumamoto University, Kumamoto, Kumamoto 860-8555, Japan
[4] Department of Earth and Planetary Science, the University of Tokyo, Hongo, Tokyo 113-0033, Japan

ABSTRACT

We investigated dehydration processes in uranyl phosphate minerals of the meta-autunite group that consist of uranyl phosphate sheets and interlayer cations, and water molecules. Meta-autunite [$Ca(UO_2PO_4)_2{\cdot}6H_2O$], metasaléeite [$Mg(UO_2PO_4)_2{\cdot}8H_2O$], and metatorbernite [$Cu(UO_2PO_4)_2{\cdot}8H_2O$] were selected for our study. The change in basal spacing between two adjacent uranyl phosphate sheets with temperature was examined by temperature-controlled X-ray diffraction (XRD) analysis from room temperature (RT) to 300 °C to determine structurally distinct, dehydrated phases. Thermogravimetric and differential thermal analyses (TG/DTA) were also performed under conditions similar to those used for the XRD analysis to clarify the hydration states of the dehydrated phases. Retention of the structure of the uranyl phosphate sheets under a high vacuum, equivalent to 300 °C, was confirmed by transmission electron microscopy. Meta-autunite, metasaléeite, and metatorbernite decreased their basal spacings by losing water molecules. Comparison of the TG/DTA and XRD results indicates that the changes in basal spacings of the dehydrated phases with temperature are as follows: 8.32 Å (6 H_2O per unit formula) at RT, 7.31 (? H_2O) and 6.68 Å (? H_2O) at 75 °C, 6.34 Å (2 H_2O) at 120 °C, and 5.81 Å (1 H_2O) at 300 °C for meta-autunite; 8.29 (8 H_2O) and 7.73 Å (? H_2O) at RT, 6.62 Å (probably, 2 H_2O) at 40 °C, 6.54 Å (2 H_2O) at 160 °C, and 5.52 Å (1 H_2O) at 300 °C for metasaléeite; and 8.61 Å (8 H_2O) at RT, 8.07 Å (4 H_2O) at 100 °C, 6.58 Å (2 H_2O) at 200 °C, and 5.60 Å (1 H_2O) at 300 °C for metatorbernite. The dehydration processes revealed by XRD and TG/DTA under similar experimental conditions are slightly different from those obtained by previous studies. Our results clearly demonstrate the presence of previously unknown dehydrated phases of the meta-autunite group minerals with basal spacings less than 6 Å that may have distinct thermodynamic properties.

INTRODUCTION

Uranium mobility in near-surface settings is mainly controlled by redox transformations between soluble hexavalent uranium [U(VI)] and insoluble tetravalent uranium [U(IV)] (Langmuir 1978; Klinkhammer and Palmer 1991; Suzuki et al. 2002, 2003, 2004a, 2004b). Reduction of U(VI) to U(IV) that occurs under reducing conditions leads to precipitation of U(IV)-bearing minerals such as uraninite, UO_{2+x}. Under oxidizing conditions, oxidative dissolution of U(IV)-bearing minerals results in mobilization of uranium due to formation of uranyl carbonate complexes (Langmuir 1978). In a wide range of uranium deposits, uranyl ions released from U(IV)-bearing minerals in primary orebodies are immobilized in insoluble uranyl phosphate minerals that persist for geological periods (Leo 1960; Snelling 1980). Nanocrystalline uranyl phosphate minerals that form during crystallization of iron oxides have been suggested to be ubiquitous (Murakami et al. 1997; Sato et al. 1997). Thus, uranyl phosphate minerals play important roles in long-term immobilization of uranium. To remediate contaminated groundwaters, sediments, and soils, technologies that enhance formation of uranyl phosphate minerals have recently drawn attention. For example, reactive barriers that use apatite [$Ca_5(PO_4)_3(F,OH)$] to promote uranyl phosphate precipitation have been studied to suppress uranium transport in groundwaters (Fuller et al. 2002). In addition, micro-organisms capable of precipitating uranyl phosphate minerals (Macaskie et al. 2000; Suzuki and Banfield 1999, 2004) have potential to be used for immobilization of uranium.

Uranyl phosphate minerals are diverse and occur in five major structural divisions, of which the autunite, meta-autunite, and the phosphuranylite groups are the most important (Finch and Murakami 1999). The autunite and meta-autunite group minerals are more important than the phosphuranylite group minerals in terms of natural abundances because of their low solubilities (Grenthe et al. 1992). The autunite and meta-autunite group minerals possess uranyl phosphate or arsenate sheets that are connected by interlayer cations and water molecules. Minerals in the autunite and meta-autunite groups are easily dehydrated by heating, desiccation, and evacuation. Thermal analysis of these minerals has been extensively conducted (Vochten et al. 1979; Vochten and Deliens 1980; Vochten and Van Doorselaer 1984; Weigel and Hoffman 1976). In contrast, few studies on structural changes associated with dehydration have

* E-mail: murakami@eps.s.u-tokyo.ac.jp

0003-004X/05/0809–1308$05.00/DOI: 10.2138/am.2005.1568

been performed. Butt and Graham (1981) reported dehydrated phases that are structurally distinct from previously identified phases by X-ray diffraction (XRD) analysis. Sverjensky (1992) indicated that the thermodynamic properties of the autunite and meta-autunite group minerals vary among the different dehydrated phases, and implied that the determination of hydration states is important. In the present study, the structural changes during dehydration caused by increasing temperature were monitored by a powder XRD device equipped with a temperature-controlling system to reveal structurally distinct, dehydrated phases. A structural change due to the high vacuum of a transmission electron microscope (TEM) was also analyzed based on selected area electron diffraction (SAED) patterns. Thermal analysis was conducted under conditions as comparable to those used for the XRD analysis as possible to clarify the hydration states of the dehydrated phases.

Crystal chemistry of meta-autunite, metasaléeite, and metatorbernite

The members of the autunite and meta-autunite groups have a general composition of $A(UO_2PO_4)_2{\cdot}nH_2O$ or $A(UO_2AsO_4)_2{\cdot}nH_2O$, where A represents a divalent cation, two monovalent cations, or some other cation(s) (A = Ca, Ba, Mg, Sr, Cu, Pb, Fe, Mn, Co, Ni, 1/2HAl, 2Na, 2K, $2NH_4$, or 2H) and *n* refers to the hydration number (Beintema 1938). For uranyl phosphate minerals of the autunite and meta-autunite groups, a uranyl phosphate sheet consists of corner-shared tetrahedra of PO_4^{3-} and square bipyramids of UO_6^{6-} (Burns et al. 1997) (Fig. 1a). Three members of the meta-autunite group, meta-autunite, metasaléeite, and metatorbernite were chosen for this study because they are often found at uranium ore deposits (Leo 1960; Snelling 1980). Dehydrated phases have been proposed for the three minerals. For example, four hydrated phases have been identified for the calcium-bearing member of the autunite and meta-autunite groups including autunite, a fully hydrated phase, and meta-autunite I, Ia, and II ("meta" means partially hydrated) (Frondel 1958; Sowder et al. 2000; Takano 1961). Unless otherwise stated, we refer to meta-autunite I as meta-autunite. Meta-autunite Ia and II have been revealed by XRD analysis at room temperature (RT) after heating to 22–50 °C and 65–150 °C, respectively.

Although the structure of autunite has recently been refined (Locock and Burns 2003a), that of meta-autunite has not yet been determined satisfactorily. Vochten and Deliens (1980) showed that meta-autunite has a tetragonal subcell with $Ca(UO_2PO_4)_2{\cdot}7H_2O$ and $a = 6.981$ and $c = 8.448$ Å while Makarov and Ivanov (1960) indicated $Ca(UO_2PO_4)_2{\cdot}6H_2O$ for the chemical composition with similar cell dimensions. Takano (1961) suggested that meta-autunite II is orthorhombic. Meta-autunite Ia has a *c* dimension of ~9 Å (Sowder et al. 2000). Saléeite, $Mg(UO_2PO_4)_2{\cdot}10H_2O$, is monoclinic. $P2_1/c$, with $\beta = 135.17°$, $a = 6.951$, $b = 19.947$, and $c = 9.896$ Å, and $Z = 2$ (Miller and Taylor 1986). The unit cell of saléeite can be recast into a pseudotetragonal setting. Metasaléeite has not been widely accepted as a separate mineral species. The name metasaléeite was proposed for the lower hydrate of saléeite by Mrose (1950) who described material from the Democratic Republic of Congo with chemical formula $Mg[(UO_2)(PO_4)]_2{\cdot}8H_2O$. Powder diffraction data for metasaléeite from Brazil were given by Cassedanne et al. (1986), PDF 41-1389, and metasaléeite has been found in central Portugal (Pinto et al. 2001). The structure of metasaléeite is currently unknown. Metatorbernite, $Cu(UO_2PO_4)_2{\cdot}8H_2O$, is tetragonal, $P4/n$, with $a = b = 6.975$ Å, $c = 17.416$ Å, and $Z = 2$ (Locock and Burns 2003b). The structural model of metatorbernite according to Locock and Burns (2003b) is shown in Figures 1a and b. The interlayer Cu^{2+} of metatorbernite is coordinated by two uranyl O atoms and by four water molecules, forming a square bipyramid as shown in Figure 1b.

Experimental procedure

The meta-autunite, metatorbernite, and metasaléeite samples were from Cunha Baxia, Portugal, Shinkolobwe, Congo, and Koongarra, Australia, respectively. The chemical states of the water molecules in meta-autunite, metatorbernite, and metasaléeite at RT were analyzed by infrared spectroscopy (IR) for each sample in a KBr pellet under ambient conditions covering the range from 4000 to 400 cm^{-1}.

Differential thermal analysis (DTA) and thermogravimetric analysis (TG) were carried out with a constant N_2 flow of 100 mL/min. To begin with, a rate of heating of 5 °C/min for the temperature range from RT to 800 °C was applied to determine the number of water molecules originally contained in the three samples. Calcium sulfate dihydrate ($CaSO_4{\cdot}2H_2O$) and magnesium sulfate heptahydrate ($MgSO_4{\cdot}7H_2O$) were used for TG standards, and showed that the measurement errors were within ±5%. A heating rate of 2.5 °C/min to 500 °C was then used with another set of three unheated samples to reveal details of the dehydration processes. For temperature-controlled XRD analysis, another set of three unheated samples was used. The samples were mounted evenly on copper slides. The samples were exposed to a constant N_2 flow of 100 mL/min for 10 min. Then, under the same N_2

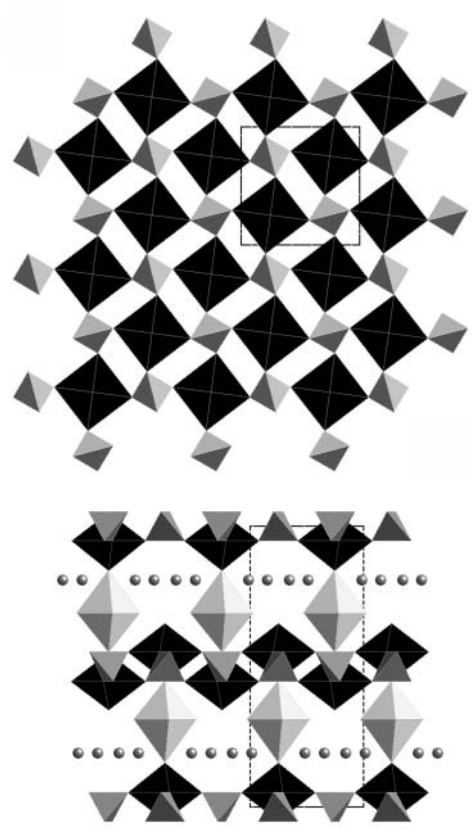

Figure 1. Crystal structure of metatorbernite according to Locock and Burns (2003b).The dashed line indicates a unit cell. A uranyl phosphate sheet consisting of corner-shared tetrahedra of PO_4^{3-} (light gray in color) and square bipyramids of UO_6^{6-} (black) is shown. The metatorbernite structure is viewed along [001] (**a**) and along [100] (**b**). Cu^{2+} ion is coordinated by two uranyl O atoms and by four water molecules, forming a square bipyramid (light gray in Fig. 1b). Water molecules not coordinating to Cu^{2+} ion are shown as gray circles.

flow, the temperature was increased to 300 °C at a rate of 2.5 °C/min. XRD patterns were obtained using a scan rate of 6 °/min at a fixed temperature with monochromatized Cu$K\alpha$ radiation at 40 kV and 30 mA. The experimental errors of the *d*-spacings determined by XRD were at most 0.04 Å.

To examine changes in the cell parameters under high vacuum, meta-autunite was observed and analyzed using a TEM equipped with energy-dispersive spectroscopy (EDS). The TEM specimens were prepared as follows: platy crystals of meta-autunite were embedded with epoxy resin and squeezed between two glass slides to orient **c*** normal to the glass slides. The glass slides were sliced parallel to **c***, and polished mechanically, and some of the slices were thinned to electron transparency by Ar ion milling and were then carbon-coated. The TEM was operated at 200 kV. SAED pattern analysis was conducted for the specimens. Chemical compositions of the three minerals were checked by EDS analysis (data deposited).

RESULTS AND DISCUSSION

Chemical states of interlayer water molecules in meta-autunite, metasaléeite, and metatorbernite

The IR spectra of metatorbernite, meta-autunite, and metasaléeite in the region of 4000 to 2500 cm^{-1} in which the absorption bands are attributed to the O-H stretching vibration are shown in Figures 2a, b, and c, respectively. There are two distinct bands at around 3350 and 2900 cm^{-1} in the spectrum of metatorbernite, while there is a single broad band at around 3400 cm^{-1} in the spectra of meta-autunite and metasaléeite. The O-H stretching frequency depends on the strength of the hydrogen bond; an increase in the strength of the hydrogen bond results in an increase in the O-H stretching frequency. In the structure of metatorbernite there are two kinds of water molecules: one coordinates to Cu^{2+} and the other does not (Locock and Burns 2003b). Because the bond strength between Cu^{2+} and the oxygen atom of a water molecule is strong due to its covalent bonding character, the strength of the hydrogen bond becomes weak. Therefore the O-H stretching band of the water molecules coordinating to Cu^{2+} is shifted toward a lower frequency, resulting in two broad bands in the region of 3700 to 2700 cm^{-1}. On the contrary, there is one broad band for metasaléeite and meta-autunite, which may indicate that the bond strength of the interlayer Cu^{2+} to the oxygen atom of a water molecule is stronger than those of Ca^{2+} and Mg^{2+}. Differences in the IR spectra other than in the region of 4000 to 2500 cm^{-1} have been described to be minor (Suzuki et al. 1998).

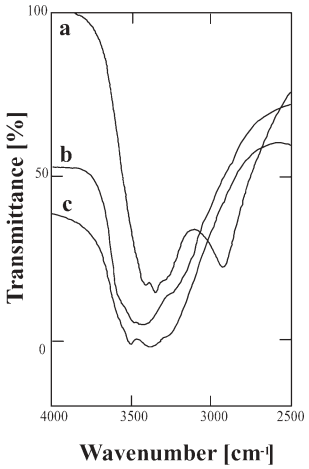

FIGURE 2. Infrared spectra of (**a**) metatorbernite, (**b**) meta-autunite, and (**c**) metasaléeite in the region of 4000 to 2500 cm^{-1} in which absorption bands are attributed to the O-H stretching vibration

Changes in hydration states during dehydration

TG and DTA curves for meta-autunite, metasaléeite, and metatorbernite in the temperature range from RT to 500 °C are shown in Figures 3a, b, and c, respectively. TG analysis up to 800 °C revealed that meta-autunite, metasaléeite, and metatorbernite contain 5.7 ± 0.3, 7.5 ± 0.4, and 8.0 ± 0.4 moles of water per unit formula, respectively. Unless otherwise stated, the hydration number of *n* water molecules with an error of 0.*m* water molecules per unit formula is hereafter referred to as *n*(*m*) H_2O, e.g., 5.7(3) H_2O.

The DTA curve of meta-autunite shows three endothermic peaks at 29, 61, and 108 °C (shown by arrows in Fig. 3a). In the TG curve, the hydration state of meta-autunite changes to 5.0(3), 3.2(2), and 2.0(1) H_2O according to the three water-loss events, respectively. After the third water-loss event at 108 °C, dehydration proceeds in a continuous manner. The DTA and TG curves of metasaléeite show two endothermic peaks at 30 and 67 °C (arrows in Fig. 3b) indicating the presence of hydration states with 5.4(3) and 3.2(2) H_2O, respectively. Above 67 °C, dehydration proceeds continuously into an anhydrous state. The DTA and TG curves of metatorbernite show two hydrate states of 6.2(3) and 4.4(2) H_2O corresponding to the two endothermic peaks at 70 and 86 °C, respectively (Fig. 3c).

Changes in structures during dehydration

To obtain more information about the dehydration processes, temperature-controlled XRD analysis was performed under condi-

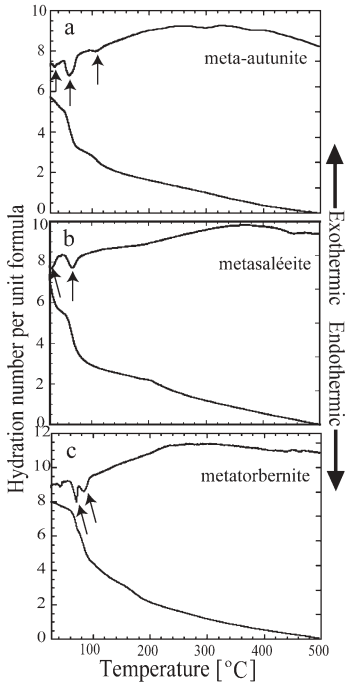

FIGURE 3. TG and DTA curves of (**a**) meta-autunite, (**b**) metasaléeite, and (**c**) metatorbernite measured from room temperature to 500 °C with a constant N_2 flow of 100 mL/min. The heating rate was 2.5 °C/min. Arrows show endothermic peaks.

tions similar to those for the thermal analysis. Representative XRD patterns of meta-autunite, metasaléeite, and metatorbernite in the temperature range RT to 300 °C are shown in Figures 4a, b, and c, respectively. Only the XRD patterns between 7.5 and 17.5° 2θ appear in Figure 4 because we only observed significant peaks in the 2θ-angle range. Because the three minerals have layered structures whose sheets are inferred to be parallel {001}, the 00*l* reflections are enhanced in powder diffraction patterns. The spacing between two adjacent uranyl phosphate sheets is referred to as the basal spacing hereafter for convenience.

The XRD pattern of meta-autunite at RT shows a reflection at 8.32(3) Å. Because Vochten and Deliens (1980) and Sowder et al. (2000) have reported that a reflection at ~8.4 Å corresponds to the basal spacing of meta-autunite, we infer that the 8.32 Å spacing is the basal spacing. While two major reflections at 7.31(2) and 6.68(2) Å were observed in the XRD pattern at 75 °C, there was only one reflection at 6.34(2) Å at 120 °C. Butt and Graham (1981) assumed that the meta-autunite reflections at 6.50 and 7.27–7.50 Å observed at 90–120 °C correspond to the basal spacings. At 300 °C, a reflection was obtained at 5.81(2) Å.

A high vacuum induces dehydration of the autunite and meta-autunite group minerals (Butt and Graham 1981). TEM specimens in which the **c*** axis of meta-autunite was oriented approximately normal to an electron beam were characterized to examine changes in the cell parameters under a high vacuum of TEM. A typical SAED pattern for meta-autunite is shown in Figure 5. Although the reflections at ~6 Å along **c*** make one diffraction spot (between the center and the 3.2 Å spot in Fig. 5), the higher-order reflections are resolved at 2.9 and 3.2 Å. The higher-order reflections at 2.9 and 3.2 Å clearly indicate that there are dehydrated phases with basal spacings of 5.8 (= 2.9 × 2) and 6.4 (= 3.2 × 2) Å under high vacuum. The 5.8 and 6.4 Å phases correspond to those with basal spacings of 5.81 Å at 300 °C and of 6.34 Å at 120 °C observed by XRD (Fig. 4a). Because the reflection at 2.9 Å is much stronger than that at 3.2 Å, meta-autunite mainly transformed into the phase with a basal spacing of 5.8 Å rather than that with a basal spacing of 6.4 Å. Thus, the reflections obtained by XRD analysis were all assigned to the basal spacings of meta-autunite.

The SAED pattern also shows that the periodicity along [110] is 4.9 Å, indicating that the *a*- and *b*-dimension of ~6.9 Å is maintained under high vacuum. That is, the structure of the uranyl phosphate sheets remains unchanged in the dehydrated phase with a basal spacing of 5.81 Å at 300 °C, which is consistent with the suggestion that the destruction of the structure of meta-autunite occurs at 600 °C (Cejka 1999).

At RT, a dominant reflection at 8.29(3) Å and a minor reflection at 7.73(3) Å were obtained for metasaléeite (Fig. 4b). At 40 °C there were three reflections at 8.23(3), 7.71(3), and 6.62(2) Å. A high peak at 6.54(2) Å was observed at 160 °C. Two reflections at 6.43(2) and 5.52(1) Å are shown in the XRD pattern at 300 °C whereas only one reflection was obtained for meta-autunite at 300 °C. We infer that as in the case of meta-autunite, the reflections in Figure 4b are attributed to the basal spacings of metasaléeite during dehydration except for one at 5.52 Å that will be discussed below.

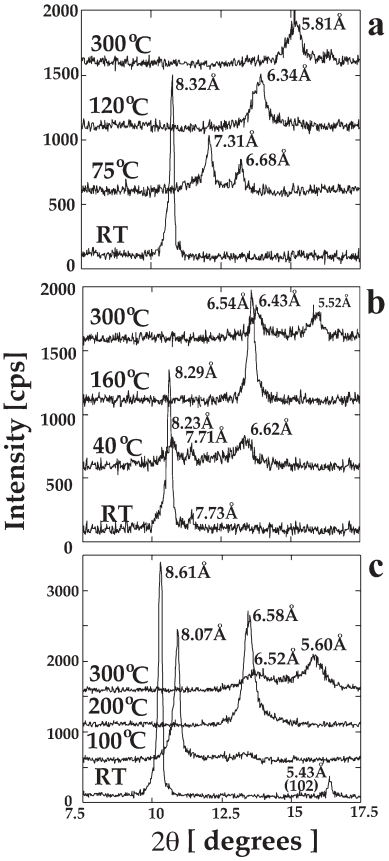

FIGURE 4. Temperature-controlled XRD patterns of (**a**) meta-autunite, (**b**) metasaléeite, and (**c**) metatorbernite observed in the temperature range from room temperature to 300 °C with a constant N_2 flow of 100 mL/min. The temperature was increased to 300 °C at a rate of 2.5 °C/min. The XRD patterns are only shown between 7.5 and 17.5° 2θ because significant peaks were observed only in this range. Experimental errors were less than 0.04 Å.

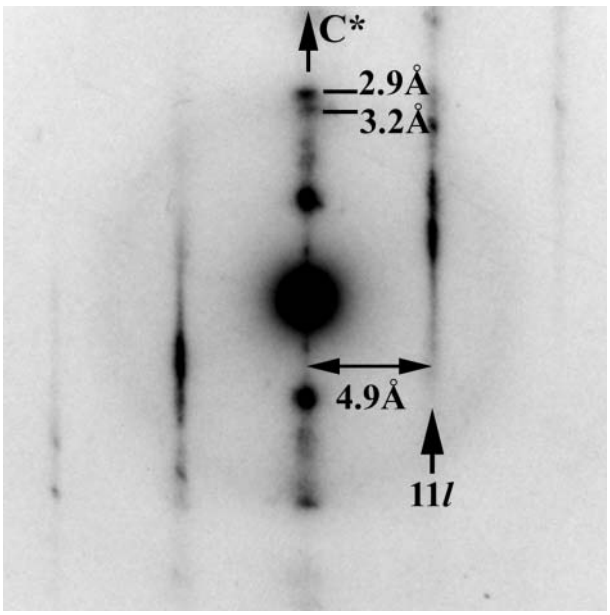

FIGURE 5. [1$\bar{1}$0] SAED pattern of meta-autunite. The specimen was prepared to orient the **c*** axis normal to the electron beam.

Metatorbernite has a major reflection at 8.61(3) Å and a minor reflection at 5.43(1) Å at RT (Fig. 4c). The 8.61 and 5.43 Å spacings are consistent with the 002 and 102 reflections of metatorbernite, respectively (Locock and Burns 2003b). At 100 and 200 °C, reflection peaks at 8.07(3) and 6.58(2) Å were obtained, respectively. There were two reflection peaks at 6.52(2) and 5.60(1) Å at 300 °C. These reflections, except those at 5.43 Å at RT and 5.60 Å at 300 °C, are inferred to correspond to the basal spacings of metatorbernite.

We will now discuss whether or not the reflections at 5.52 and 5.60 Å for metasaléeite and metatorbernite, respectively, at 300 °C correspond to basal spacings. The reflections with basal spacings of ~6.5 Å occurring at 160 and 200 °C for metasaléeite and metatorbernite, respectively, are slightly shifted and lose intensity at 300 °C when the reflections at ~5.5 Å appear (Figs. 4b and 4c). This suggests that the dehydrated phases with basal spacings of ~6.5 Å lose their domains and other phases that have spacings of ~5.5 Å grow at 300 °C. Although the 00*l* reflections are enhanced, the peaks at ~5.5 Å show broadening similar to the meta-autunite peak at 5.81 Å (Fig. 4) that was confirmed to be a basal spacing by TEM (Fig. 5). We may occasionally have *hkl* reflections even for oriented samples as shown by the 102 reflection of metatorbernite at RT (Fig. 4c). Because the TEM observations revealed that the structure of the uranyl phosphate sheets is retained, we can roughly calculate the d_{102}-spacing at 300 °C. The maximum d_{102}-spacing at 300 °C is calculated to be ~4.8 Å if 6.6 Å, a basal spacing of metatorbernite at 200 °C (Fig. 4c), is a maximum basal spacing at 300 °C. The value of ~4.8 Å is significantly smaller than the value of ~5.5 Å appearing at 300 °C. The above consideration leads us to the interpretation that the metasaléeite and metatorbernite reflections at 5.52 and 5.60 Å, respectively, at 300 °C correspond to basal spacings.

Hydration of structurally distinct phases occurring during dehydration

In this section, we attempt to clarify the hydration states of structurally distinct phases occurring during dehydration by combining the results of the XRD and thermal analyses. First, it should be noted that there is a limit to accurate comparison between the XRD and TG/DTA results because perfectly identical experimental conditions were impossible to produce in the different instruments. In addition, a few stages of dehydration proceed simultaneously, that is, a few dehydrated phases co-exist at a given temperature (Fig. 4) although TG/DTA analysis provides one hydration state at a given temperature. Therefore, hydration numbers of the structurally distinct phases were carefully estimated from the results obtained by TG/DTA. The basal spacings revealed by XRD and the corresponding hydration numbers by TG/DTA are tabulated in Table 1, where XRD data from some previous studies are also given.

We will compare the hydration numbers of the structurally distinct phases for the present study to those from previous studies below. However, most previous studies presented either XRD or TG/DTA data but not both. In addition, because the experimental conditions are different, changes in basal spacing and hydration state with temperature for the present study do not precisely correspond to those for the previous studies. Therefore, the comparison will be carefully discussed.

Meta-autunite. At RT, meta-autunite has a basal spacing of 8.32 Å (Fig. 4a) and a hydration state of 5.7(3) H_2O (Fig. 3a), close to 6 H_2O. We can interpret that meta-autunite with a basal spacing of 8.32 Å has 6 H_2O. However, the value of 8.32 Å is slightly smaller than that of ~8.4 Å given by Vochten and Deliens (1980) and Sowder et al. (2000), and a hydration number of 6 to 7 H_2O is suggested for meta-autunite (Sowder et al. 2000).

There are two dehydrated phases with basal spacings of 7.31 and 6.68 Å at 75 °C (Fig. 4a). The DTA curve shows a water-loss event at 61 °C that corresponds to a hydration state of 3.2(2) H_2O by TG (Fig. 3a). Because meta-autunite has two dehydrated phases that do not occur at other temperatures and the TG curve is steep at around 60 °C, we failed to determine the hydration numbers of the dehydrated phases at 7.31 and 6.68 Å at 75 °C.

The dehydrated phase with a basal spacing of 6.34 Å at 120 °C was observed by XRD analysis (Fig. 4a). The thermal analysis shows an endothermic peak at 108 °C corresponding to the presence of a hydration number of 2.0(1) H_2O (Fig. 3a). Because the endothermic peak ends at ~120 °C, the dehydrated phase with a basal spacing of 6.34 Å is formed by this water-loss event. Thus, the hydration state of the dehydrated phase with a basal spacing of 6.34 Å at 120 °C is 2 H_2O.

Meta-autunite has a dehydrated phase with a basal spacing of 5.81 Å at 300 °C (Fig. 4a), which was confirmed by SAED (Fig. 5). The TG curve of meta-autunite shows 1.0(1) H_2O for the hydration number at 300 °C and a continuous decrease from 300 to 500 °C (Fig. 3a). We therefore interpret that the dehydrated phase contains 1 H_2O.

The basal spacings of meta-autunite revealed by XRD for the present study are in good agreement with those of Butt and Graham (1981): 7.31 and 6.68 Å at 75 °C correspond to the 7.50 and 6.54 Å at 90 °C of Butt and Graham (1981), and 6.34 Å at 120 °C to the 6.50 Å at 120 °C of Butt and Graham (1981) as shown in Table 1. This agreement suggests that the ~7.4 and ~6.5 Å dehydrated phases are relatively stable. We did not observe meta-autunite Ia or II (Takano 1961; Vochten and Deliens 1980; Sowder et al. 2000) in the present study. The TG data of Sowder et al. (2000) suggest the presence of dehydrated phases with 2, 1, and 0 H_2O at ~90, ~160, and ~240 °C, respectively. In contrast, our results show that the dehydrated phases with 2 and 1 H_2O occur at 120 and 300 °C, respectively, and lose water continuously up to 500 °C (Fig. 3a).

Metasaléeite. Metasaléeite has a basal spacing of 8.29 Å at RT (Fig. 4b), and the thermal analysis shows the hydration state is 7.5(4) H_2O (Fig. 3b) at RT. Because there is another phase with a smaller basal spacing, 7.73 Å, and with much less intensity at RT (Fig. 4b), the phase with a basal spacing of 8.29 Å probably has 8 H_2O. In contrast, Frost and Weier (2004) suggested 7 H_2O for the hydration state of metasaléeite. We failed to determine the hydration state of the phase with a basal spacing of ~7.7 Å that also appears at 40 °C (Fig. 4b).

There are three peaks at 8.23, 7.71, and 6.62 Å at 40 °C (Fig. 4b). We interpret that the dehydrated phase at 8.23 Å is a remnant of the phase at 8.29 Å at RT because of the decrease in intensity and slight peak-shift with increase in temperature. Similarly, the dehydrated phase at 6.62 Å is possibly a precursor of the phase at 6.54 Å at 160 °C (Fig. 4b). The hydration state of the phase with a basal spacing of ~7.7 Å is not known.

At 160 °C the dehydrated phase at 6.54 Å has a single and relatively strong peak (Fig. 4b). The TG curve shows that the cor-

TABLE 1. Basal spacings and estimated hydration states of dehydrated phases of meta-autunite, metasaléeite, and metatorbernite

T (°C)	meta-autunite			metasaléeite		metatorbernite	
	B. S.*	H. S.†	B. S.(R)‡	B. S.	H. S.	B. S.	H. S.
RT	8.32(3)	6	9.02§	8.29(3)	8	8.61(3)	8
RT			8.74‖	7.73(3)	?		
RT			8.47**				
RT			8.41#				
RT			8.43§				
RT			8.16**				
RT			8.10§				
40				8.23(3)	8		
40			8.49‖	7.71(3)	?		
40				6.62(2)	2?		
60			8.41‖				
75	7.31(2)	?					
75	6.68(2)	?					
90			7.50‖				
90			6.54‖				
100						8.07(3)	4
120	6.34(2)	2	7.27‖				
120			6.50‖				
160				6.54(2)	2		
200						6.58(2)	2
300	5.81(2)	1		6.43(2)	2?	6.52(2)	2?
300				5.52(1)	1	5.60(1)	1

* Basal spacing (angstroms in unit) with error in parentheses as revealed by XRD analysis in the present study.
† Hydration state of meta-autunite, metasaléeite or metatorbernite during dehydration. The hydration number of *n* water molecules with the uncertainty of *m* water molecules per unit formula is designated as $n(m)$ H_2O.
‡ Basal spacings of dehydrated phases reported in the references below.
§ Data from Sowder et al. (2000). The 9.02 Å phase is meta-autunite Ia at RT cooled from up to 50 °C, the 8.43 Å phase meta-autunite I at RT from up to 70 °C, and the 8.10 Å phase meta-autunite II at RT from up to 150 °C.
‖ Data from Butt and Graham (1981).
Data from Vochten and Deliens (1980).
** Data from Takano et al. (1961). The 8.47 Å phase is meta-autunite I at RT, dried after being soaked in water, and the 8.16 Å phase meta-autunite II at RT cooled from 110 °C.

responding hydration state is 2.5(1) H_2O (Fig. 3b). Consequently, the dehydrated phase contains 2 or 3 H_2O. As discussed below, some portion of the dehydrated phase at 6.54 Å at 160 °C persists at 300 °C together with a further dehydrated phase at 5.52 Å (Fig. 4b), and the hydration state is ~1 H_2O at 300 °C (Fig. 3b). In addition, the dehydrated phases Å of meta-autunite and metatorbernite with basal spacings of 6.3–6.6 have 2 H_2O (Table 1). We infer that the hydration state of the dehydrated phase at 6.54 Å is 2 H_2O rather than 3 H_2O.

There are two dehydrated phases with basal spacings of 6.43 and 5.52 Å at 300 °C for metasaléeite (Fig. 4b). The dehydrated phase at 6.43 Å is a remnant of the phase at 6.54 Å at 160 °C because of the decrease in intensity and slight peak-shift with increase in temperature. The TG curve shows that the hydration state is slightly higher than 1 H_2O at 300 °C (Fig. 3b) where the dehydrated phases at 6.43 and 5.52 Å occur. Therefore, the dehydrated phase at 5.52 Å has either 1 or 0 H_2O. A recent study of metasaléeite revealed that a dehydrated phase with 2 H_2O loses 1 H_2O at 231 °C, and loses 1 H_2O at 376 °C to become anhydrous (Frost and Weier 2004). In addition to the results of Frost and Weier (2004), the TG curve shows that metasaléeite loses water continuously from 300 to 500 °C. We interpret that the dehydrated phase at 5.52 Å contains 1 H_2O.

Frost and Weier (2004) indicated by thermal analysis that saléeite (10 H_2O) dehydrates into 7, 4, 2 and 1 H_2O phases at ~40, ~70, ~90, and ~230 °C, respectively, and finally becomes anhydrous at ~380 °C. We observed dehydrated phases of metasaléeite with 2 H_2O at 160 °C and with 1 H_2O at 300 °C. The two results are consistent in terms of the dehydration process, but not in terms of the temperatures of formation. The presence of a dehydrated phase with 2 H_2O at 193 °C shown by Vochten and Van Doorselaer (1984) is consistent with our results.

Metatorbernite. Our metatorbernite has a basal spacing of 8.61 Å and 8.0(4) H_2O at RT (Figs. 4c and 3c, respectively), which is in good agreement with the data of Locock and Burns (2003b).

Metatorbernite has a dehydrated phase with a distinct peak at 8.07 Å at 100 °C (Fig. 4c). The DTA curve shows an endothermic peak at 86 °C and the hydration number revealed by TG is 4.4(2) H_2O at 100 °C where the endothermic peak ends (Fig. 3c). Hence, the dehydrated phase with a basal spacing of 8.07 Å is formed by this water-loss event, and contains 4 or 5 H_2O. In the structure of metatorbernite, water molecules coordinate to Cu^{2+} more strongly than those to Ca^{2+} and Mg^{2+} as discussed above and the four water molecules coordinating to Cu^{2+} (Fig. 1b) are considered to be retained during dehydration. This inference is supported by the high intensity of the peak at 8.07 Å at 100 °C. Therefore, the dehydrated phase with a basal spacing of 8.07 Å most probably contains 4 H_2O.

The dehydrated phase of metatorbernite with a basal spacing of 6.58 Å at 200 °C was observed by XRD analysis (Fig. 4c). The intensity of the 6.6 Å peak is not so strong as those at 8.61 or 8.07 Å, but is significantly strong. The TG data shows that a dehydrated phase contains 2.1(1) H_2O at 200 °C (Fig. 3c). We infer that the hydration state of the dehydrated phase is 2 H_2O.

There are dehydrated phases with basal spacings of 6.52 and 5.60 Å at 300 °C for metatorbernite (Fig. 4c). We interpret that the dehydrated phase at 6.52 Å is a remnant of the phase at 6.58 Å at 200 °C because of the decrease in intensity and slight peak-shift with increase in temperature. Therefore, the dehydrated phase at ~6.5 Å probably has 2 H_2O. At 300 °C, the TG curve shows that the hydration state is slightly higher than 1 H_2O (Fig. 3c), which may be due to co-existence of the 6.52 Å phase with the 5.60 Å one (Fig. 4c). Metatorbernite loses water continuously from 300 to 500 °C. Therefore, we infer that the phase at 5.60 Å at 300 °C has 1 H_2O.

Vochten et al. (1981) showed by TG/DTA that metatorbernite with 8 H_2O dehydrates to 4, 2, and 0 H_2O phases at 120, 150, and 150–450 °C, respectively, which is almost consistent with our results except that a 1 H_2O phase occurs in the present study.

We have shown the hydration states of structurally distinct phases during dehydration of meta-autunite, metasaléeite, and metatorbernite by temperature-controlled XRD and TG/DTA. The present results are unique because the dehydrated phases are presented with both basal spacings and hydration numbers. The presence of previously unknown dehydrated phases with basal spacings less than 6 Å has been demonstrated for the first time in the present study.

ACKNOWLEDGMENTS

The authors are indebted to P.L. Airey, P. Duerden, A.A. Snelling, and M. Deliens for providing the samples. M. Saigo is acknowledged for her assistance with the XRD analysis. This manuscript was greatly improved by the comments of P.C. Burns and an anonymous reviewer. The electron microscopy was performed in the Electron Microbeam Analysis Facility of the Department of Earth and Planetary Science, the University of Tokyo. Part of the present study was supported by the Grant-in-Aid program of the Ministry of Education, Culture, Sports, Science and Technology to T.M.

REFERENCES CITED

Beintema, J. (1938) On the composition and crystallography of autunite and the meta-autunites. Recueil des Travaux Chimiques des Pays-Bas, 57, 155–175.

Burns, P.C., Ewing, R.C., and Hawthorne, F.C. (1997) The crystal chemistry of hexavalent uranium: Polyhedron geometries, bond-valence parameters, and polymerization of polyhedra. Canadian Mineralogist, 35, 1551–1570.

Butt, C.R.M. and Graham, J. (1981) Sodian potassian hydrooxonian meta-autunite: first natural occurrence of an intermediate member of a predicted solid series. American Mineralogist, 66, 1068–1072.

Cassedanne, J.P., Cassedanne, J.O., and De Carvalho, H.F. (1986) Loellingite, uraninite, and their alteration products in the pegmatite from Urucum (Minas Gerais, Brazil). Academia Brasileira de Ciências, 58, 249 266.

Cejka, J. (1999) Infrared spectroscopy and thermal analysis of the uranyl minerals. In S.A.T. Redfern and M.A. Carpenter, Eds., Transformation Processes in Minerals, 38, 521–622. Reviews in Mineralogy and Geochemistry, Mineralogical Society of America, Washington, D.C.

Finch, R. and Murakami, T. (1999) Systematics and paragenesis of uranium minerals. In S.A.T. Redfern and M.A. Carpenter, Eds., Transformation Processes in Minerals, 38, 91–179. Reviews in Mineralogy and Geochemistry, Mineralogical Society of America, Washington, D.C.

Frondel, C. (1958) Systematic mineralogy of uranium and thorium. Geological Survey Bulletin, 1064, 400p. U.S. Government Printing Office, Washington.

Frost, R.L. and Weier, M.L. (2004) Hot-stage Raman spectroscopic study of the thermal decomposition of saléeite. Journal of Raman Spectroscopy, 35, 299–307.

Fuller, C.C., Bargar, J.R., Davis, J.A., and Piana, M.J. (2002) Mechanisms of uranium interactions with hydroxyapatite: Implications for groundwater remediation. Environmental Science and Technology, 36, 158–165.

Grenthe, I., Fuger, J., Konnigs, R.J.M., Lemire, R.J., Muler, A.B., Nguyen-Trung, C., and Wanner, H. (1992) Chemical thermodynamics of uranium, 715 p. In H. Wanner and I. Forest, Eds., Chemical Thermodyanmics, vol. 1. Elsevier, Amsterdam.

Klinkhammer, G.P. and Palmer, M.R. (1991) Uranium in the oceans: where it goes and why. Geochimica et Cosmochimica Acta, 55, 1799–1806.

Langmuir, D. (1978) Uranium solution-mineral equilibria at low temperatures with applications to sedimentary ore deposits. Geochimica et Cosmochimica Acta, 42, 547–569.

Leo, G.W. (1960) Autunite from Mt. Spokane. American Mineralogist, 45, 99–128.

Locock, A.J. and Burns, P C. (2003a) The crystal structure of synthetic autunite, $Ca[(UO_2)(PO_4)]_2(H_2O)_{11}$. American Mineralogist, 88, 240–244.

——— (2003b) Crystal structures and synthesis of the copper-dominant members of the autunite and meta-autunite groups: torbernite, zeunerite, metatorbernite and metazeunerite. Canadian Mineralogist, 41, 489–502.

Macaskie, L.E., Bonthrone, K.M., Young, P., and Goddard, D.T. (2000) Enzymatically mediated bioprecipitation of uranium by *Citrobacter* sp.: A concerted role for exocellular lipopolysaccharide and associated phosphatase in biomineral formation. Microbiology, 146, 1855–1867.

Makarov, Y.S. and Ivanov, I. (1960) The crystal structure of metaautunite, $Ca[UO_2PO_4]_2 \cdot 6H_2O$. Doklady Akademii Nauk, SSSR, 135, 673–676.

Miller, S.A. and Taylor, J.C. (1986) The crystal structure of saléeite, $Mg[UO_2PO_4]_2 \cdot 10H_2O$. Zeitschrift für Kristallographie, 177, 247–253.

Mrose, M.E. (1950) Studies of uranium minerals (III): Saléeite from Schneeberg, Saxony. American Mineralogist, 35, 525–530.

Murakami, T., Ohnuki, T., Isobe, H., and Sato, T. (1997) Mobility of uranium during weathering. American Mineralogist, 82, 888–899

Pinto, M.M.S.C., Silva, M.M.V.G., and Neiva, A.M.R. (2001) Uranium mineralization and water contamination in Central Portugal. Water-Rock Interaction, Proceedings of the International Symposium on Water-Rock Interaction, 10th, Villasimius, Italy, 2, 1261–1264.

Sato, T., Murakami, T., Yanase, N., Isobe, H., Payne, T.E., and Airey, P.L. (1997) Iron nodules scavenging uranium from groundwater. Environmental Science and Technology, 31, 2854–2858.

Snelling, A.A. (1980) Uraninite and its alteration products, Koongarra uranium deposit. In J. Ferguson and A.B. Goleby, Eds., Uranium in the Pine Creek Geosyncline, p. 487–498. International Atomic Energy Agency, Vienna.

Sowder, A.G., Clark, S.B., and Fjeld, R.A. (2000) Dehydration of synthetic autunite hydrates. Radiochimica Acta, 88, 533–538.

Suzuki, Y. and Banfield, J.F. (1999) Geomicrobiology of uranium. In S.A.T. Redfern and M.A. Carpenter, Eds., Transformation Processes in Minerals, 38, 393–432. Reviews in Mineralogy and Geochemistry, Mineralogical Society of America, Washington, D.C.

——— (2004) Resistance to and accumulation of uranium by bacteria from a uranium-contaminated site. Geomicrobiology Journal, 21, 113–121.

Suzuki, Y., Murakami, T., Kogure, T., Isobe, H., and Sato, T. (1998) Crystal chemistry and microstructures of uranyl phosphates. Material Research Society Symposium Proceedings, 506, 839–846. The Material Research Society, Pittsburgh, PA.

Suzuki, Y., Kelly, S.D., Kemner, K.M., and Banfield J.F. (2002) Nanometer-size products of uranium bioreduction. Nature, 419, 134.

——— (2003) Microbial populations stimulated for hexavalent uranium reduction in uranium contaminated sediment. Applied and Environmental Microbiology, 69, 1337–1346.

——— (2004a) Enzymatic U(VI) reduction by *Desulfosporosinus* species. Radiochimica Acta, 92, 11–16.

——— (2004b) Direct microbial reduction and subsequent preservation of uranium in natural near-surface sediment. Applied and Environmental Microbiology, 71, 1790–1797.

Sverjensky, D. (1992) Geochemical modeling of secondary uranium ore formation. Alligator Rivers Analogue Project Final Report 11, DOE/HMIPRP/92/081, 51 p. Australian Nuclear Science and Technology Organisation, Sydney.

Takano, Y. (1961) X-ray study of autunite. American Mineralogist, 46, 812–822.

Vochten, R. and Deliens, M. (1980) Transformation of curite into meta-autunite. Paragenesis and electrokinetic properties. Physics and Chemistry of Minerals, 6, 129–143.

Vochten, R. and Van Doorselaer, M. (1984) Secondary uranium minerals of the Cunha Baxia Mine. The Mineralogical Record, 15, 293–297.

Vochten, R., Huybrechts, W., Remaut, G., and Deliens, M. (1979) Formation of meta-torbernite starting from curite: Crystallographic data and electrokinetic properties. Physics and Chemistry of Minerals, 4, 281–290.

Vochten, R., Piret, P., and Goeminne, A. (1981) Synthesis, crystallographic data, solubility and electrokinetic properties of copper-, nickel- and cobalt-uranylphosphate. Bulletin de Minéralogie, 104, 457–467.

Weigel, F. and Hoffman, G. (1976) The phosphates and arsenates of hexavalent actinides. Part I. Uranium. Journal of the Less-Common Metals, 44, 99–123.

MANUSCRIPT RECEIVED DECEMBER 2, 2003
MANUSCRIPT ACCEPTED DECEMBER 8, 2004
MANUSCRIPT HANDLED BY PETER BURNS